Cell-specific mitotic defect and dyserythropoiesis associated with erythroid band 3 deficiency

Barry H. Paw[1,11], Alan J. Davidson[1], Yi Zhou[1], Rong Li[2], Stephen J. Pratt[1], Charles Lee[3], Nikolaus S. Trede[1], Alison Brownlie[1,11], Adriana Donovan[1], Eric C. Liao[1], James M. Ziai[1], Anna H. Drejer[1], Wen Guo[1], Carol H. Kim[4], Babette Gwynn[5], Luanne L. Peters[5], Marina N. Chernova[6], Seth L. Alper[6], Agustin Zapata[7], Sunitha N. Wickramasinghe[8], Matthew J. Lee[8], Samuel E. Lux[1], Andreas Fritz[9], John H. Postlethwait[10] & Leonard I. Zon[1]

Published online 31 March 2003; doi:10.1038/ng1137

Most eukaryotic cell types use a common program to regulate the process of cell division. During mitosis, successful partitioning of the genetic material depends on spatially coordinated chromosome movement and cell cleavage[1]. Here we characterize a zebrafish mutant, *retsina* (*ret*), that exhibits an erythroid-specific defect in cell division with marked dyserythropoiesis similar to human congenital dyserythropoietic anemia. Erythroblasts from *ret* fish show binuclearity and undergo apoptosis due to a failure in the completion of chromosome segregation and cytokinesis. Through positional cloning, we show that the *ret* mutation is in a gene (*slc4a1*) encoding the anion exchanger 1 (also called band 3 and AE1), an erythroid-specific cytoskeletal protein. We further show an association between deficiency in Slc4a1 and mitotic defects in the mouse. Rescue experiments in *ret* zebrafish embryos expressing transgenic *slc4a1* with a variety of mutations show that the requirement for band 3 in normal erythroid mitosis is mediated through its protein 4.1R–binding domains. Our report establishes an evolutionarily conserved role for band 3 in erythroid-specific cell division and illustrates the concept of cell-specific adaptation for mitosis.

The *ret* mutation was originally identified in a chemical mutagenesis screen for morphological and developmental mutants. Two independent alleles with identical phenotype, *tr217* and *tr265*,

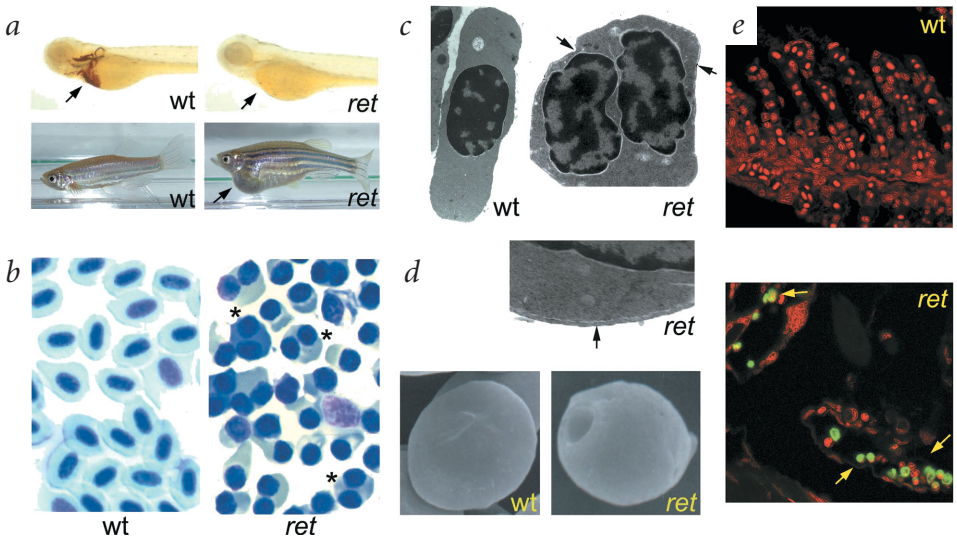

Fig. 1 Analysis of the phenotype associated with the *ret* mutation. **a**, Wild-type (wt) and *ret* embryos 72 h post-fertilization (hpf; upper panels) were stained with o-dianisidine to detect hemoglobinized cells in the cardiac sinus (arrows). Severe anemia in the *ret* embryo was indicated by the absence of o-dianisidine staining. Affected *ret* embryos had normal embryonic erythropoiesis until 72 hpf when profound anemia became evident. An adult *ret* zebrafish showed growth retardation, pallor and gross cardiomegaly (arrow) from severe chronic anemia (lower panel). **b**, Peripheral blood cells from wild-type (wt) zebrafish compared with concentrated peripheral blood cells from *ret* fish. Binucleated *ret* erythroblasts are indicated by asterisks. Other hematopoietic lineages appear grossly unaffected with a normal complement of monocytes, neutrophils and lymphocytes, indicating a specific role for *ret* in normal erythropoiesis. **c**, Transmission electron micrographs of wild-type (wt) and *ret* erythroblasts. The *ret* erythroblasts showed binuclearity (right) and greater peripheral cisternae (arrows). Lower panel shows a higher magnification of the peripheral cisternae from a *ret* erythroblast. **d**, Scanning electron micrographs from wild-type (wt) and *ret* erythroblasts showed discoid and abnormal spherical shapes, respectively. **e**, Paraffin sections from gill regions of wild-type (wt) and *ret* adult fish stained for apoptotic erythroid cells in capillaries by TUNEL assay. TUNEL-positive cells are green and are indicated by arrows. The specificity of apoptosis was confirmed by absence of TUNEL-staining in non-hematopoietic organs.

[1]*Department of Medicine, Division of Hematology-Oncology, Children's Hospital; Department of Pediatric Oncology, Dana-Farber Cancer Institute; Howard Hughes Medical Institute, Children's Hospital; and Department of Pediatrics, Harvard Medical School, Boston, Massachusetts, USA.* [2]*Department of Cell Biology, Harvard Medical School, Boston, Massachusetts, USA.* [3]*Department of Pathology, Brigham & Women's Hospital and Harvard Medical School, Boston, Massachusetts, USA.* [4]*Department of Biochemistry, Microbiology and Molecular Biology, University of Maine, Orono, Maine, USA.* [5]*The Jackson Laboratory, Bar Harbor, Maine, USA.* [6]*Molecular Medicine and Renal Units, Beth Israel Deaconess Medical Center, and Department of Medicine, Harvard Medical School, Boston, Massachusetts, USA.* [7]*Department of Cell Biology, Complutense University, Madrid, Spain.* [8]*Nuffield Department of Clinical Laboratory Sciences, University of Oxford, John Radcliffe Hospital, Oxford, UK and Department of Hematology, Imperial College of Science, Technology and Medicine, St. Mary's Campus, London, UK.* [9]*Department of Biology, Emory University, Atlanta, Georgia, USA.* [10]*Institute of Neuroscience, University of Oregon, Eugene, Oregon, USA.* [11]*Present addresses: Division of Hematology-Oncology, Brigham & Women's Hospital, Boston, Massachusetts, USA (B.H.P.); XenonGenetics, Vancouver, British Columbia, Canada (A.B.). Correspondence should be addressed to L.I.Z. (e-mail: zon@rascal.med.harvard.edu).*

were identified as causing anemia (Fig. 1*a*; ref. 2). The autosomal recessive mutation is lethal for most mutant embryos; the few embryos that survive to adulthood show signs of chronic anemia (Fig. 1*a*). Analysis of histological preparations of peripheral blood and of kidney from *ret* adult fish indicates a differentiation arrest at the late erythroblast stage with roughly 27% binuclearity (Fig. 1*b*), suggesting a defect in cytokinesis. The dysplastic features are reminiscent of the binucleated erythroid precursors in humans with congenital dyserythropoietic anemia (CDA) type II (OMIM 224100; refs. 3,4). This rare disorder is representative of the more common dyserythropoiesis observed in bone marrow during stress from pre-leukemia or infection. The high percentage of binucleated erythroid cells in *ret* mutants is unusual among the zebrafish blood mutants. For instance, mutants with defects in erythroid β-spectrin, *riesling*[5], and protein 4.1R, *chablis* or *merlot*[6], have less than 1% binucleated cells yet have comparably severe anemia. This suggests a specific defect in mitosis associated with the *ret* mutation.

Transmission electron micrographs of erythroblasts from the *tr265* allele showed binucleated cells with 'double membranes,' or peripheral cisternae from more endoplasmic reticulum, in roughly 11% of the binucleated cells (Fig. 1*c*). This ultrastructural feature is another hallmark of erythroid progenitors from individuals with CDA type II[7]. Scanning electron micrographs showed an abnormal spherical shape of *ret* erythroblasts compared with the biconcave-shaped erythrocytes from wild-type fish (Fig. 1*d*). Erythroblasts from both *ret* alleles underwent programmed cell death (Fig. 1*e*). No differences were detected between wild-type and *ret* erythroblasts stained with antibody against phosphorylated histone H3, a marker of cells in mitosis phase[8], thereby excluding lower proliferation rate as an etiology for the anemia in *ret* erythroblasts (data not shown).

To gain further insight into the *ret* defect, we used a positional cloning strategy to identify the disrupted gene. The *ret* locus was mapped using linkage analysis with simple-sequence length polymorphism markers[9]. Bulk segregant analysis localized *ret* to zebrafish linkage group 3, 0.2 cM (5 recombinants per 2,240 meioses) from marker *z1140*. A chromosomal walk initiated from *z1140* identified a critical P1-derived artificial chromosome (PAC) clone 233G13 encompassing the *ret* locus (Fig. 2*a*). We used direct PAC hybridization on a kidney cDNA library and recovered a clone which encoded a partial cDNA for the erythroid anion exchanger 1 (*slc4a1*), encoding band 3. The erythrocyte band 3 is composed of two distinct domains: a cytoplasmic N terminus involved in interaction with cytoskeletal proteins and a transmembrane C terminus involved in anion exchange[10].

We identified mutations in *slc4a1* in the *ret* alleles. In *tr265*, we identified an A→G transition at position 1476, which results in the substitution of glycine for glutamic acid at residue 456 (E456G, corresponding mouse sequence, Glu491; Fig. 2*b*). In *tr217*, we identified an insertion of 13 nucleotides (GTGGCTGTAATCA) in the cDNA at nucleotide 503, predicting a frame shift and premature translation termination (Fig. 2*b*). Analysis of the genomic sequence from *tr217* identified a T→G transversion near the 3′ end of intron 5, activating a new splice-acceptor site. The gene *slc4a1* is deleted in the deficiency allele, *b245*, which lacks a large segment of linkage group 3 (Fig. 2*c*; ref. 11).

Whole-mount *in situ* hybridization to embryos showed that *slc4a1* was expressed in a tissue-restricted pattern in the intermediate cell mass (Fig. 2*d*), an organ equivalent to the site of embryonic hematopoiesis in higher vertebrates. The expression of early hematopoietic genes, such as *gata1* (Fig. 2*d*), *lmo2* and *scl* (data not shown), is unaffected in *ret* embryos 24 hours after fertilization.

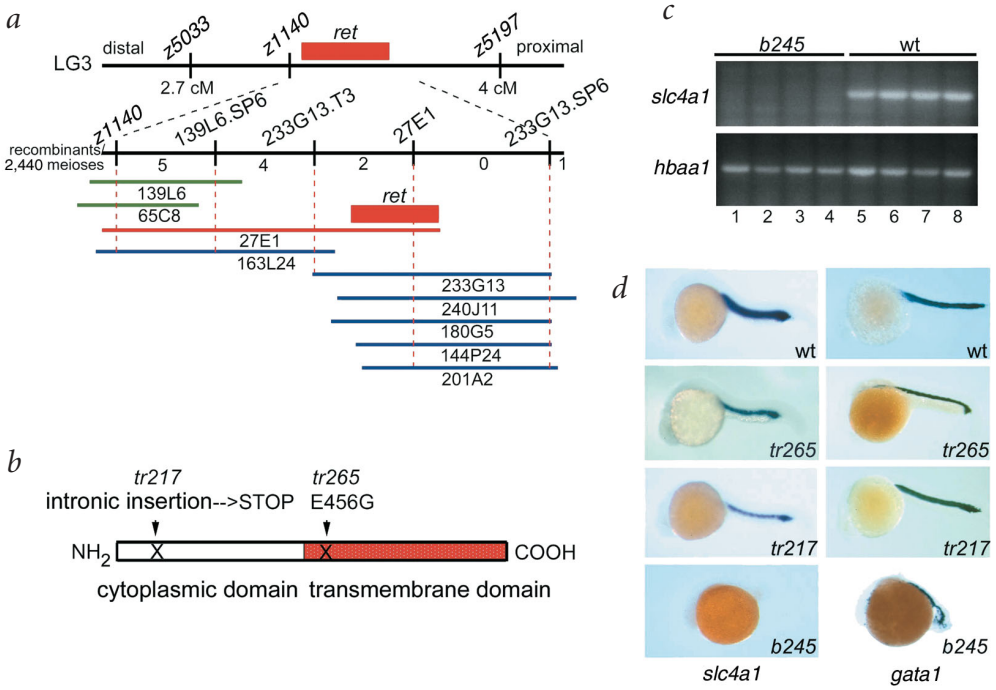

Fig. 2 Analysis of the *ret* locus and expression pattern. ***a***, Genetic and physical map of the *ret* region. 'Distal' and 'proximal' refer to telomere and centromere, respectively. A number of genes already positioned on linkage group 3 suggest an orthologous relationship to human chromosome 17q. The human *SLC4A1* locus maps to chromosome 17q21–22, consistent with the zebrafish ortholog *slc4a1* being the gene mutated in *ret*. ***b***, Schematic model of the protein encoded by *ret*. The band 3 protein has an N-terminal cytoplasmic domain for protein–protein interactions and a C-terminal transmembrane domain (shown in red) for anion exchange. The zebrafish band 3 protein has an overall amino-acid identity of roughly 50% with both human and mouse band 3 proteins and amino-acid identity of roughly 70% with trout and salmon band 3. The locations of mutations identified in *ret* alleles are indicated by arrows. RT–PCR was done on RNA from *tr217* embryos, confirming that the activated splice-acceptor site was used exclusively over the endogenous splice acceptor. The identified mutations were confirmed by ASO hybridization on genomic DNA. ***c***, The *ret* locus is deleted in the *b245* deficiency allele. Mutant embryos (lanes 1–4) and wild-type siblings (wt; lanes 5–8) were tested for the presence of *slc4a1* and control *hbaa1* loci. ***d***, Whole-embryo *in situ* hybridization on 24-hpf embryos showing expression of *slc4a1* and *gata1* in the hematopoietic intermediate cell mass. The expression of *slc4a1* is altered in *ret* embryos as compared with wild-type (wt) embryos, with slightly reduced levels in *tr265*, reduced levels in *tr217* and complete absence in *b245*. The reduced level of *slc4a1* transcripts in *tr217* is consistent with nonsense-mediated mRNA decay.

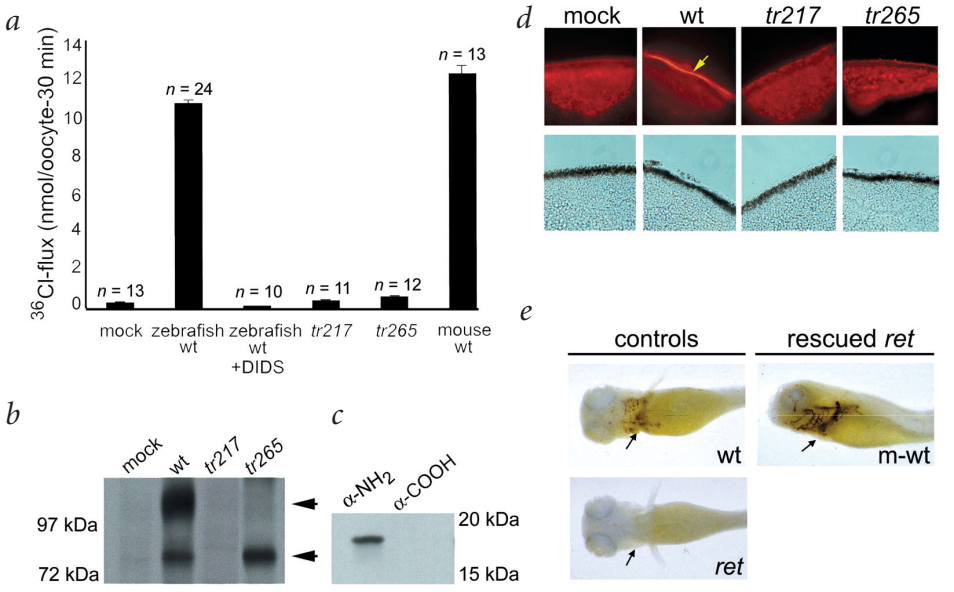

Fig. 3 Functional analysis of the protein encoded by *ret*. **a**, ^{36}Cl flux activity of *slc4a1* cRNAs expressed in *X. laevis* oocytes. Mock indicates oocytes that were injected with buffer; +DIDS indicates oocytes that were co-incubated with a pharmacologic inhibitor of *slc4a1* (DIDS). wt, wild-type. **b**, Immunoprecipitation of *X. laevis* oocytes expressing zebrafish *slc4a1* cRNAs with antisera against N-terminal band 3. The extensive N-glycan modification on wild-type band 3 protein is represented by the band at $M_r \cong 110$ kDa. The high-mannose conjugate of the band 3 protein is represented by the band at $M_r \cong 80$ kDa. **c**, Immunoprecipitation of the truncated mutant protein encoded by *tr217* with antisera against the N terminus (α-NH_2) but not the C terminus (α-COOH). **d**, Immunolocalization of zebrafish band 3 protein (rhodamine; arrow) at the cell surface of *X. laevis* oocytes (top panels). Phase-contrast views of cryosections are shown in the bottom panels. Mock indicates oocytes that were injected with buffer. wt, wild-type. **e**, Partial rescue of anemic *ret* embryos by mouse *Slc4a1* cRNA expression. Control wild-type (wt) and *ret* embryos and rescued *ret* embryos (m-wt) were stained with o-dianisidine to detect hemoglobin in the cardiac sinus and gills (arrows). The criterion for rescue was >50 hemoglobinized red cells per embryo, in contrast to the baseline complete absence of hemoglobinized cells in *ret* mutants.

We studied the functional consequences of these mutations on anion transport by expressing *slc4a1* cRNA in *Xenopus laevis* oocytes and assaying for uptake of ^{36}Cl (Fig. 3*a*). Injections with *slc4a1* or mouse *Slc4a1* cRNA resulted in 40–60 times greater influx of ^{36}Cl than mock injection controls. Anion flux activity by zebrafish band 3 is abolished by preincubation with 4,4′-diisothiocyanostilbene-2,2′-disulfonate (DIDS), a specific covalent inhibitor of band 3 anion transport[10]. Injections with *tr265* or *tr217* cRNAs showed no flux activity.

Metabolic labeling with [^{35}S]-methionine of *X. laevis* oocytes injected with zebrafish wild-type *slc4a1* cRNA followed by immunoprecipitation showed extensive post-translational, N-linked glycosylation (Fig. 3*b*). Digestion with peptide-N-glycosidase F confirmed the extensive N-glycan modification acquired by the wild-type band 3 protein (data not shown). In contrast, mutant band 3 protein from *tr265* showed no extensive post-translational modification (Fig. 3*b*), indicating that the mis-folded protein is retained in the rough–endoplasmic reticulum compartment by the cellular quality-control machinery. We confirmed the truncated band 3 polypeptide ($M_r \cong 18$ kDa) predicted by the *tr217* allele by selective immunoprecipitation with antisera recognizing the N terminus but not the C terminus (Fig. 3*c*). Immunolocalization of band 3 in cryosectioned *X. laevis* oocytes injected with wild-type *slc4a1* cRNA showed correct targeting of the normal zebrafish protein to the cell surface (Fig. 3*d*). In contrast, both mutant band 3 proteins did not localize in the plasma membrane.

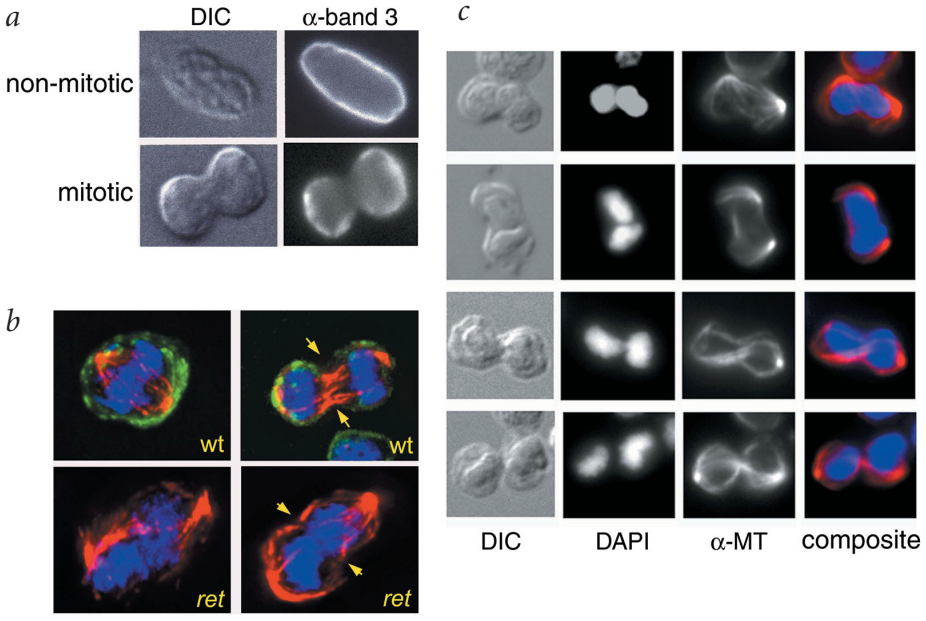

Fig. 4 Role of band 3 in erythroid cytokinesis. **a**, Immunolocalization of band 3 on wild-type erythroblasts during nonmitotic and mitotic phases of the cell cycle. α-band 3, antisera against band 3; DIC, differential interference contrast. **b**, Comparison of band 3 (green), microtubules (red) and DNA (blue) in wild-type (wt) and *ret* erythroblasts. Cleavage furrow (arrows) could initiate in normal and mutant cells but further ingression was blocked in *ret* cells by chromosomes (blue) that did not segregate to the polar regions. The images were collected on a DeltaVision optical sectioning microscope. Shown are flattened three-dimensional views after deconvolution and compression of the optical sections. **c**, Abnormally oriented mitotic spindles were noted in binucleated erythroblasts from *ret* mutants. Shown are images of erythroblast cellular outline (DIC), nuclei (DAPI; blue) and immunostained microtubules (α-MT; red).

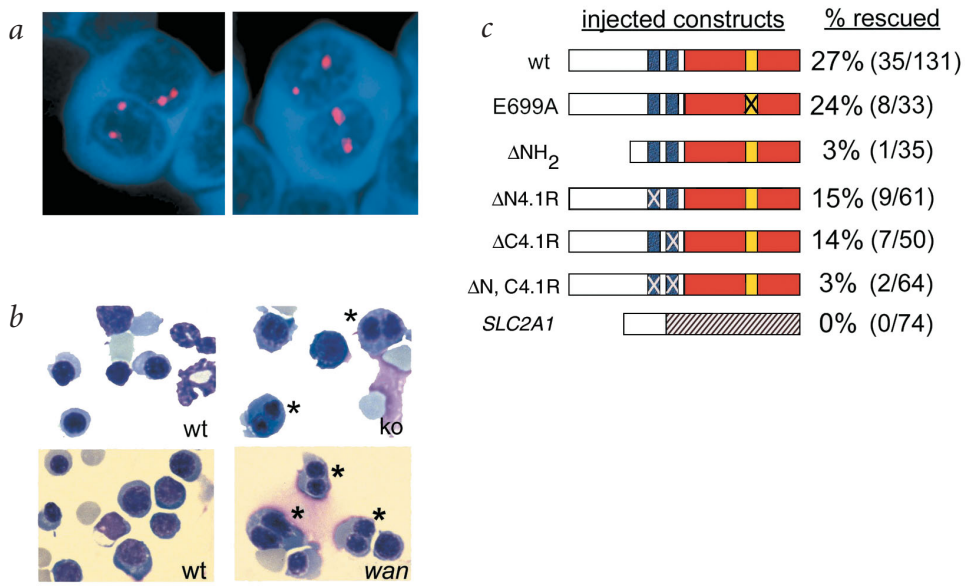

Fig. 5 Erythroid cytokinesis defect in mouse and zebrafish band 3 mutants and structure–function relationship of mouse band 3 for rescuing anemia in *ret* embryos. ***a***, FISH analysis of binucleated erythroblasts from *ret* zebrafish showing a total of four rhodamine (red) signals for a genomic DNA probe from linkage group 3, suggesting that these cells were tetraploid. Cells were counterstained with DAPI. ***b***, Fetal liver and spleen smears from 18-d.p.c. wild-type (wt), homozygous *Slc4a1* knockout (ko) and *wan/wan* (*wan*) mice are depicted. Binucleated erythroblasts are marked with asterisks. ***c***, Rescue of *ret* embryos by mouse *Slc4a1* or human *SLC2A1* cRNA expression. Schematic models of the mouse *Slc4a1* constructs are depicted: cytoplasmic domain, white; transmembrane domain, red; two protein 4.1R–interaction domains, blue; and amino-acid residue 699 involved in anion transport, yellow. Mutated sequences in the protein 4.1R–binding domains or amino-acid residue 699 are indicated by an 'X'. The transmembrane domain of the human *SLC2A1* is depicted by striped bar. Using differential interference contrast optics, examination of *ret* fish rescued by band 3 injection showed erythroid cells with elliptical shape and a single nucleus; therefore, expression of wild-type (wt) *Slc4a1* cRNA rescues the mitotic defect in *ret* embryos.

We attempted transient transgenic rescues of anemic *ret* embryos by injection with either *slc4a1* or mouse *Slc4a1* cRNA. Injection of *Slc4a1* cRNA into mutant embryos at the 1–2 cell stage partially rescued the anemia in 27% of the *ret* mutant embryos ($n = 131$; Fig. 3*e*). Injection of wild-type zebrafish *slc4a1* cRNA into mutant *ret* embryos partially rescued the anemia in 19% ($n = 68$; data not shown) of the *ret* embryos; in contrast, ectopic expression of zebrafish *slc4a1* cRNA harboring the *tr265* allele did not rescue mutant embryos from anemia ($n = 57$; data not shown). Taken together, these data indicate that the *ret* mutation is caused by defects in *slc4a1*.

The binucleated morphology of *ret* erythroblasts compelled us to investigate the role of band 3 in normal erythroid cell division. We studied the subcellular localization of band 3 in normal zebrafish erythroblasts by immunohistochemistry. In non-mitotic erythroblasts, band 3 was localized circumferentially around the cell (Fig. 4*a*). In contrast, mitotic erythroblasts excluded band 3 from the cleavage furrow and concentrated it to the cortical polar regions (Figs. 4*a*,*b*). Band 3 was absent from the membrane surface of *ret* erythroblasts (Fig. 4*b*). In mutant erythroblasts, although the cleavage furrow could initiate (Fig. 4*b*), further ingression was prohibited by chromosome masses that did not segregate to the poles, resulting in binucleated cells. Staining for microtubules also identified defects in spindle structure in mitotic *ret* erythroblasts (Fig. 4*c*); in particular, there was a reduction of the overlapping microtubules in the spindle midzone (Fig. 4*b*). Therefore, the cell-division defect in *ret* erythroblasts may be because band 3 is required for proper segregation of the chromosomes during anaphase instead of having a direct role in formation of the cleavage furrow. Non-erythroid tissues in *ret* mutants do not have cytokinesis defects, because band 3 is expressed exclusively in erythrocytes and kidney. Fluorescence *in situ* hybridization (FISH) analysis of *ret* erythroblasts with a zebrafish genomic probe showed that the binucleated cells were tetraploid (Fig. 5*a*).

To investigate whether band 3 is involved in erythroid cytokinesis of other vertebrates, we analyzed fetal liver and spleen erythroblasts from mice lacking band 3 because of targeted gene disruption[12] or the spontaneous null mutation *wan*[13] (Fig. 5*b*). Homozygous *wan* embryos had roughly 14% binucleated erythroblasts, compared with roughly 2% binucleated erythroblasts in wild-type and heterozygous siblings. *Slc4a1* knockout fetuses had roughly 4% binucleated erythroblasts, compared with <1% binucleated cells in normal siblings. The difference in severity of binuclearity and phenotype between the mouse mutants possibly reflects a strain-specific dominant modifier in the *Slc4a1* background[13]. The role of band 3 in normal erythroid cytokinesis is thus conserved throughout vertebrate evolution.

To address the contribution of the anion exchange function of band 3 in normal erythroid cytokinesis, we examined whether mutant band 3 proteins would rescue anemia when expressed in *tr217* embryos. Specific mutations in *Slc4a1* that result in the amino-acid substitutions E699A[14] and E699Q[15] ablated monovalent anion transport function; however, these mutant band 3 proteins still folded and integrated into the cell surface membrane. Injections of mouse wild-type *Slc4a1* cRNA or *Slc4a1* cRNA encoding E699A/E699Q mutant band 3 partially rescued the anemia in *ret* embryos (Fig. 5*c* and data not shown). Therefore, the structural features of band 3, not its ion translocation function, are crucial for erythroid cytokinesis.

We generated a series of mutant mouse band 3 constructs to further define the structural domains involved in cytokinesis. To address the structural contribution of the cytoplasmic domain in erythroid cytokinesis, we expressed a mutant band 3 protein that lacks most of the N terminus (ΔNH_2) but still integrates into the plasma membrane in *tr217* embryos. Absence of the band 3 cytoplasmic domain greatly diminished its ability to rescue the anemia in mutant embryos (Fig. 5*c*).

Members of the protein 4.1 family have been shown to interact with band 3; for instance, the versatile adapter protein 4.1R has been shown to interact with band 3 domains containing the amino-acid motifs LRRRY (N4.1R, amino-acid residues 356–360) and IRRRY (C4.1R, amino-acid residues 405–409; refs. 16–18). The interaction sites for band 3 and protein 4.1R in

mammalian proteins also exist in the corresponding zebrafish band 3 (IRY versus IKRRY) and protein 4.1R (LEEDY versus LERDY; ref. 6). To address the contribution of protein 4.1R interaction domains in erythroid cytokinesis, we mutated these conserved motifs to AAAAA singly (ΔN4.1R, ΔC4.1R) or in combination (ΔN,C4.1R). Ablation of either protein 4.1R–binding site alone could still partially rescue anemia in *ret* embryos, but ablation of both sites in band 3 greatly diminished its ability to rescue *ret* embryos (Fig. 5*c*). Taken together, these data indicate that the structural role of band 3 in normal erythroid cytokinesis is mediated by its N-terminal cytoplasmic domain and requires at least one intact protein 4.1R–binding site at the juxtamembrane. Given the ubiquity of protein 4.1R in many cellular processes, it was surprising that a more severe loss-of-function phenotype was not observed in mouse and zebrafish null mutants. Several protein 4.1 family members are expressed in developing tissues. The viable and milder phenotype of the mouse[19] and zebrafish protein 4.1R[6] mutants suggest that there is partial compensation by other protein 4.1 family members for red-cell development[19].

Because band 3 constitutes the largest proportion of the integral membrane proteins in erythrocytes, it is possible that the nonspecific lack of integral membrane proteins and resultant membrane loss might explain the *ret* cytokinesis defects. To exclude this possibility, we expressed another integral membrane protein in erythrocytes, human glucose transporter 1 (GLUT1, encoded by *SLC2A1*), in *ret* embryos. GLUT1 did not rescue anemia (Fig. 5*c*), arguing that band 3 has a specific role in erythroid cytokinesis.

Protein 4.1R isoforms, which interact directly with band 3 in erythroid cells, reside in interphase cells near the plasma membrane, in the nuclear matrix[20] and in association with centrosomes[21]. Protein 4.1R also interacts with the nuclear mitotic apparatus protein and with dynein and dynactin, which are involved in spindle assembly and organization during mitosis[22]. Ectopic expression of the actin-binding domain of protein 4.1R or its C terminus disrupts mitotic spindles *in vitro*[23] and *in vivo*[24]. We speculate that band 3 serves as the point on the erythroblast cell cortex to which the poles of the spindle attach through interaction of astral microtubules with protein 4.1R or another yet uncharacterized bridging protein. Such interactions may be important for efficient spindle elongation and the completion of chromosome segregation. Alternatively, band 3 could more directly effect chromosome segregation.

Although one CDA type II locus has been mapped to human chromosome 20q11.2 in French and Italian pedigrees[25], severe forms of CDA type II do not map to 20q11.2 (ref. 26), indicating molecular heterogeneity. Our analyses of exonic sequences from ten index cases with clinically mild CDA did not identify mutations in *SLC4A1* (data not shown). It is nonetheless possible that a subset of individuals with severe type II dyserythropoietic anemia have mutations in *SLC4A1*. Our studies of *slc4a1* deficiency in zebrafish and mouse along with the abnormal N-glycan processing[3] and anion exchange activity[27] of band 3 in human CDA type II strongly suggest its contributory role in the pathophysiology of dyserythropoiesis. In the absence of proper band 3 assembly in the cytoskeleton of developing erythroblasts, mitotic defects arise and apoptosis ensues. The gene associated with CDA type II on human 20q11.2 may be involved either in processing of band 3 to the cell surface or in association of band 3 with the mitotic apparatus. This same pathway might be affected in other dyserythropoietic conditions when the marrow is stressed, such as those resulting from infection or pre-leukemia.

Methods

Zebrafish strains. We recovered alleles *tr217* and *tr265* mutagenized with N-ethyl-N-nitrosourea from a screen in Tübingen, Germany[2]. We recovered the deficiency allele *b245* in Eugene, Oregon[11]. We maintained *ret* fish on standard genetic AB background. Polymorphic strains used for genetic mapping were DAR, SJD and WIK.

Genetic mapping, chromosomal walk and cDNA selection. We collected diploid mutant and wild-type embryos from hybrid AB/DAR, AB/SJD and AB/WIK heterozygotes. We used genome-wide scanning on bulk segregant pooled DNA for linkage analysis[9]. We genotyped individual embryos with simple sequence length polymorphism markers *z1140* and *z5197* (ref. 9). We used genetic marker *z1140* to isolate BAC, PAC and YAC clones for assembling a physical contig through the *ret* locus. We isolated the PAC233G13 insert DNA and hybridized it to an arrayed cDNA library as described[28]. We recovered a partial *slc4a1* cDNA clone containing nucleotides 1,680–2,815 (amino acids 521–902) and then used it to screen an oligo-dT-primed adult-kidney cDNA library in λZap Express for a full-length cDNA clone.

Mutational analysis and allele-specific oligonucleotide (ASO) hybridization. We isolated total RNA from mutants 4 d post-fertilization (dpf). We generated cDNA by reverse transcription and PCR amplification in four overlapping fragments, which we subcloned for sequencing analysis. To confirm the missense *tr265* and *tr217* alleles, we amplified genomic DNA with primers and analyzed the PCR product by ASO hybridization[29] with either wild-type or mutant oligonucleotides. Primer sequences for amplification and ASO hybridization are available on request.

Zebrafish whole-embryo *in situ* hybridization and o-dianisidine staining. We carried out whole-embryo *in situ* hybridizations with *gata1* and *slc4a1* essentially as described[2]. We stained live embryos 4 dpf with o-dianisidine (Sigma) as described[2].

cRNA injections and constructs. We subcloned an *Eco*RI fragment of zebrafish *slc4a1* cDNA into the pCS2+ vector. We filled in the *Eco*RI–*Hin*dIII fragment of mouse *slc4a1* cDNA with T4 DNA polymerase and blunt-end ligated it into the *Stu*I site of pCS2+. We generated cDNA constructs containing the zebrafish alleles (*tr217* and *tr265*) and mouse alleles (encoded the E699A and E699Q mutant band 3 proteins) by QuikChange site-directed mutagenesis (Stratagene). The sequence motifs LRRRY (N4.1R, amino-acid residues 356–360) and IRRRY (C4.1R, amino-acid residues 405–409), the protein 4.1R–interacting domains in mouse band 3, were mutated to AAAAA as either single (ΔN 4.1R, ΔC 4.1R) or double (ΔN,C 4.1R) combinations by QuikChange mutagenesis. We generated a construct deleting much of the mouse band 3 cytoplasmic domain (ΔNH_2) by introducing an artificial Kozak sequence and an initiator methionine site at Glu338. Each mutant construct was expressed in HEK293 cells by transient transfection; targeting of each mutant protein to the plasma membrane was documented by immunohistochemistry with an antibody recognizing the C terminus of mouse band 3. We subcloned the *Bam*HI fragment of *SLC2A1* into pCS2+. We prepared cRNA from linearized plasmids using the SP6 mMessage Machine kit (Ambion). Fertilized eggs from *tr217* heterozygous pairs were injected at the 1–2 cell stage with roughly 100 pg *slc4a1* or *SLC2A1* cRNA. Injected embryos were allowed to develop to 4 dpf, stained with o-dianisidine and genotyped by ASO hybridization after photo-documentation.

Antibodies. We generated antisera directed against zebrafish band 3 amino-acid residues 90–105 of the N-terminal cytoplasmic domain (C-WQETGRWVGFEENFS) and against the 14 C-terminal amino-acid residues (C-LDADDANVKFDDED) in rabbits (Genemed Synthesis). We affinity-purified the antisera against the immunizing peptides. The antibody against mouse band 3 was directed against the 12 C-terminal amino acids[12]. We purchased the antibody against phosphorylated histone H3 from Upstate Biotechnology.

Immunohistochemistry. We cultured *X. laevis* oocytes injected with wild-type and mutated zebrafish *slc4a1* cRNAs for 48–60 h at 18 °C in ND96 medium as described[15]. We sequentially incubated 8-μm-thick

cryosections of oocytes in a solution containing 1× phosphate-buffered saline, 1% bovine serum albumin, 10% heat-inactivated bovine serum for 1 h at room temperature, washed them three times with 1× phosphate-buffered saline, incubated them with affinity-purified antibody against N-terminal band 3 (1:100 dilution) for 1 h, washed them three times and incubated them with rhodamine-conjugated antibody again rabbit immunoglobin (1:100 dilution) for 1 h.

We dissected out the kidneys from wild-type or *ret* fish. We generated a single-cell suspension by mechanical pipetting and fixed the cells in 4% paraformaldehyde at room temperature for 20 min, washed them in phosphate-buffered saline and applied them to polylysine-coated coverslips. We immunostained erythroid cells in this cell suspension with antisera against band 3 as above. We also stained the erythroid cells with monoclonal antisera against tubulin (Sigma) and counterstained them with DAPI (Molecular Probes).

Immunoprecipitation. We metabolically labeled injected *X. laevis* oocytes with Trans^{35}S-label (approximately 1000 Ci mmol^{-1}, ICN) in ND96 medium for 2 d at 18 °C. We carried out immunoprecipitation essentially as described[15] using affinity-purified antisera against band 3.

Anion flux assay. We carried out ^{36}Cl-flux (^{36}Cl as NaCl, 12 mCi g^{-1}; ICN) assays of injected *X. laevis* oocytes (stages V–VI) as described[15].

Apoptotic TUNEL staining. We stained paraffin-embedded sections of wild-type and *ret* fish using the Apoptosis Detection System, Fluorescein (Promega).

Scanning and transmission electron microscopy. We collected blood from wild-type and *ret* fish and processed it for scanning electron microscopy as described[12]. We carried out transmission electron microscopy on sectioned fish as described[4].

Mouse strains. We used mice with a targeted disruption of *Slc4a1* (ref. 12) and a spontaneous *Slc4a1*-null mutant, C3H/HeJ-*wan*[13], which have been described. We dissected fetal liver and spleen from homozygous mutant and wild-type littermates 18 d post-coitum (d.p.c.) and stained cytospins of the mechanically minced fetal liver and spleen with Wright-Giemsa. We used residual mouse fetal tissue for genotyping as described[12,13].

FISH analysis. We prepared kidney cells from juvenile *ret* zebrafish for FISH according to manufacturer's recommendations (Bioview). We labeled a genomic DNA probe for linkage group 3, Zf3C5G, with rhodamine-11-dUTP, hybridized it and washed it according to standard procedures (Bioview). We captured images on an Olympus AX70 fluorescence microscope using Applied Imaging Genus software.

GenBank accession number. Zebrafish *slc4a1*, AF350072.

Acknowledgments

We thank K. Dooley, C. Burns, D. Ransom, D. Traver, L. Washburn and C. Birkenmeier for critical review of the manuscript; P. Haffter and C. Nüsslein-Volhard for providing the WIK strain; C. Amemiya, A. Schier and W. Talbot for support and advice; S. Johnson for the DAR and SJD strains; M. Mueckler for SLC2A1 cDNA; M. Listewnik for assistance with the FISH experiments; and N. White and W. Saganic for the zebrafish husbandry. B.H.P. was supported by a Howard Hughes Medical Institutes Post-doctoral Fellowship for Physicians and the US National Institutes of Health. L.I.Z. is an Investigator of the Howard Hughes Medical Institutes. L.L.P. was supported by a US National Cancer Institute Cancer Core Grant to The Jackson Laboratory. The work was supported by funding from the US National Institutes of Health.

Competing interests statement

The authors declare that they have no competing financial interests.

Received 11 November 2002; accepted 7 March 2003.

1. Field, C., Li, R. & Oegema, K. Cytokinesis in eukaryotes: a mechanistic comparison. *Curr. Opin. Cell. Biol.* **11**, 68–80 (1999).
2. Ransom, D.G. *et al*. Characterization of zebrafish mutants with defects in embryonic hematopoiesis. *Development* **123**, 311–319 (1996).
3. Fukuda, M.N. Congenital dyserythropoietic anaemia type II (HEMPAS) and its molecular basis. *Baillieres Clin. Haematol.* **6**, 493–511 (1993).
4. Wickramasinghe, S.N. Congenital dyserythropoietic anaemias: clinical features, haematological morphology and new biochemical data. *Blood Rev.* **12**, 178–200 (1998).
5. Liao, E.C. *et al*. Hereditary spherocytosis in zebrafish *riesling* illustrates evolution of erythroid β-spectrin structure, and function in red cell morphogenesis and membrane stability. *Development* **127**, 5123–5132 (2000).
6. Shafizadeh, E. *et al*. Characterization of zebrafish *merlot/chablis* as a non-mammalian vertebrate model for severe hereditary elliptocytosis due to protein 4.1 deficiency. *Development* **129**, 4359–4370 (2002).
7. Alloisio, N. *et al*. The cisternae decorating the red blood cell membrane in congenital dyserythropoietic anemia (type II) originating from the endoplasmic reticulum. *Blood* **87**, 4433–4439 (1996).
8. Wei, Y. *et al*. Phosphorylation of histone H3 is required for proper chromosome condensation and segregation. *Cell* **97**, 99–109 (1999).
9. Knapik, E.W. *et al*. A microsatellite genetic linkage map for zebrafish (*Danio rerio*) *Nat. Genet.* **18**, 338–343 (1998).
10. Handin, R.I., Lux, S.E. & Stossel, T.P. *Blood: Principles and Practice of Hematology.* (J.P. Lippincott, Philadelphia, 1995).
11. Fritz, A., Rozowski, M., Walker, C. & Westerfield, M. Identification of selected gamma-ray induced deficiencies in zebrafish using multiplex polymerase chain reaction. *Genetics* **144**, 1735–1745 (1996).
12. Peters, L.L. *et al*. Anion exchanger 1 (band 3) is required to prevent erythrocyte membrane surface loss but not to form the membrane skeleton. *Cell* **86**, 917–927 (1996).
13. Peters L.L. *et al*. Failure of effective reticulocytosis in a new spontaneous band 3 deficient mouse strain (C3H/HeJ-*wan*) and in a subset of targeted band 3 null mice (B6,129 AE1–/–) suggests the presence of genetic modifiers of band 3 function in red blood cells. *Blood* **92** Suppl. 1, 301 (1998).
14. Sekler, I., Lo, R.S. & Kopito, R.R. A conserved glutamate is responsible for ion selectivity and pH dependence of the mammalian anion exchangers AE1 and AE2. *J. Biol. Chem.* **270**, 28751–28758 (1995).
15. Chernova, M.N. *et al*. Electrogenic sulfate/chloride exchange in *Xenopus* oocytes mediated by murine AE1 E699Q. *J. Gen. Physiol.* **109**, 345–360 (1997).
16. Jons, T. & Drenckhahn, D. Identification of the binding interface involved in linkage of cytoskeletal protein 4.1 to erythroid anion exchanger. *EMBO J.* **11**, 2863–2867 (1992).
17. An, X-L. *et al*. Modulation of band 3-ankyrin interaction by protein 4.1. *J. Biol. Chem.* **271**, 33187–33191 (1996).
18. Lombardo, C.R., Willardson, B.M., Low, P.S. Localization of the protein 4.1-binding site on the cytoplasmic domain of erythrocyte membrane band 3. *J. Biol. Chem*. **267**, 9540–9546 (1992).
19. Shi, Z-T. *et al*. Protein 4.1R-deficient mice are viable but have erythroid membrane skeleton abnormalities. *J. Clin. Invest.* **103**, 331–340 (1999).
20. Krauss, S.W. *et al*. Structural protein 4.1 in the nucleus of human cells: dynamic rearrangements during cell division. *J. Cell. Biol.* **137**, 275–289 (1997).
21. Krauss, S.W. *et al*. Structural protein 4.1 is located in mammalian centrosomes. *Proc. Natl. Acad. Sci. USA* **94,** 7297–7302 (1997).
22. Mattagajasingh, S.N. *et al*. A nonerythroid isoform of protein 4.1R interacts with the nuclear mitotic apparatus (NuMA) protein. *J. Cell. Biol.* **145**, 29–43 (1999).
23. Krauss, S.W. *et al*. Two distinct domains of protein 4.1 critical for assembly of functional nuclei *in vitro*. *J. Biol. Chem.* **277,** 44339–44346 (2002).
24. Perez-Ferreiro, C.M. *et al*. 4.1R protein associate with interphase microtubules in human T cells. *J. Biol. Chem.* **276**, 44785–44791 (2001).
25. Gasparini, P. *et al*. Localization of the congenital dyserythropoietic anemia II locus to chromosome 20q11.2 by genome-wide search. *Am. J. Hum. Genet*. **61**, 1112–1116 (1997).
26. Iolascon, A. *et al*. Genetic heterogeneity of congenital dyserythropoietic anemia type II. *Blood* **92**, 2593–2594 (1998).
27. De Franceschi, L. *et al*. Decreased band 3 anion transport activity and band 3 clusterization in congenital dyserythropoietic anemia type II. *Exp. Hematol.* **26**, 869–873 (1998).
28. Brownlie, A. *et al*. Positional cloning of the zebrafish sauternes gene: a model for congenital sideroblastic anaemia. *Nat. Genet.* **20**, 244–250 (1998).
29. Farr, C.J., Saiki, R.K., Erlich, H.A., McCormick, F. & Marshall, C.J. Analysis of RAS gene mutations in acute myeloid leukemia by polymerase chain reaction and oligonucleotide probes. *Proc. Natl. Acad. Sci. USA* **85**, 1629–1633 (1988).